ABSTRACT

Title of Thesis: **Sutureless Anastomosis: Electroadhering a Hydrogel Sleeve Over Cut Pieces of Tubular Tissue**
Samantha Marie Grasso, Master of Science, 2024

Directed By: Prof. Srinivasa R. Raghavan
Department of Chemical & Biomolecular Engineering

Recently, our lab demonstrated that cationic gels could be adhered to animal tissues by applying an electric field (10 V DC, for ~ 20 s). This phenomenon, termed electroadhesion (EA), could potentially be used to repair injured tissues without sutures. An extreme injury is when a tube in the body (e.g., a blood vessel or an intestine) is cut into two segments. The surgical process of joining the segments is termed anastomosis, and thus far has only been done clinically with sutures. Here, we explore the use of EA for performing sutureless anastomoses *in vitro* with bovine aorta and chicken intestine. For this purpose, we make a strong and stretchable cationic gel in the form of a sleeve (i.e., a hollow tube). By using a custom plastic mold, we control both the sleeve diameter and wall thickness. A sleeve with a diameter matching that of the tubular tissue is slipped over the cut segments of the tube, followed by application of the DC electric field. Thereby, the sleeve becomes strongly adhered by EA to the underlying tube. Water or blood is then flowed through the repaired tube, and we record the burst pressure P_{burst} of the tube. We find that P_{burst} is > 80 mm Hg and close to the P_{burst} of an intact (uncut) tube. In comparison to the sleeve, a long strip of the gel attached around the cut tubular pieces allows a much lower P_{burst}. Thus, our study shows that gel-sleeves adhered by EA could enable anastomoses to be performed in the clinic without the need for sutures.

Sutureless Anastomosis: Electroadhering a Hydrogel Sleeve Over Cut Pieces of Tubular Tissue

By

Samantha Marie Grasso

Thesis submitted to the Faculty of the Graduate School of the
University of Maryland, College Park, in partial fulfillment
of the requirements for the degree of
Master of Science
2024

Advisory Committee:

Prof. Srinivasa R. Raghavan, Dept. of Chemical & Biomolecular Engineering, Chair

Prof. Taylor Woehl, Dept. of Chemical & Biomolecular Engineering

Prof. Nam S. Wang, Dept. of Chemical & Biomolecular Engineering

© Copyright by
Samantha Marie Grasso
2024

Dedication

This thesis is dedicated to my mom and dad. Thank you for the 23 years of unwavering love and support.

Acknowledgements

I would like to first express my gratitude to my advisor, Dr. Raghavan, for his constant support and guidance over the past three years. As both a professor and mentor, I hold Dr. Raghavan in very high esteem and am honored to have been one of his students. Throughout my journey in this program, he has been a continuous source of encouragement, consistently acknowledging my potential and nurturing me into the scientist I am today. I have gained invaluable skills under his mentorship that I will carry with me through future endeavors.

I want to thank my thesis committee: Dr. Wang and Dr. Woehl. Dr. Wang's generosity and patience have proved to be invaluable, dedicating so much of his time to walk me through Numerical Methods. Additionally, I thank my collaborators, Dr. Anthony Sandler and Dr. Sarah Wright at Children's National Hospital, for sharing their knowledge of medical expertise and granting us access to their animal facility. Working alongside such brilliant surgeons has been a humbling experience.

I want to thank my mentor, Dr. Leah Borden, with whom I had the privilege of working with during my undergraduate studies. I consider myself immensely fortunate to have received Leah's guidance and witnessed her journey in founding her own company centered on electroadhesion. Leah's confidence, elegance, and compassion have deeply imprinted on me. As I navigate my path in the world, I aspire to emulate these admirable qualities she embodies.

I am eternally grateful to my colleagues in the Raghavan lab, whose friendships have enriched my experience. Paula Montero has grown into my big sister, always looking over me. Paula made every day brighter, and the idea of seeing her ignited my enthusiasm. Paula's wit and brilliance enabled her to swiftly resolve issues that had stumped me for months. Having spent almost two years with Paula, my intellect has been sharpened, and my confidence has grown. I am also equally grateful to Morine Nader for her unwavering support. Morine never hesitated to prioritize my needs above her own, both personally and professionally. Her selflessness is remarkable, and I am fortunate to have her as a colleague and friend. I also want to express my gratitude to Eylul Utlu. Our friendship is special in my heart because Eylul's unwavering adoration, loyalty, and acceptance of me have never been more deeply felt in any other friendship. I would also like to thank Faraz, Mahima, Wenaho, Irene, Ireene, and Wei-Yei for their friendships, which I will forever cherish.

I would also like to thank my best friend, Sarangua Battamur, for being by me throughout this journey and infusing me with life. Your motivation and passion have left a lasting imprint on me, and I couldn't imagine celebrating this victory with anyone else. I would also like to thank Caroline Stuart, Lucy Hughes, Ben Robinson, Lena Akil, Laura Marhefka, Pedram Chehreghani, and Jordan La for the friendships we formed as undergrads in the engineering program.

Finally, I want to express my gratitude to my family at L'Ardente. Every Monday, I counted the days until I would return to the restaurant. This job revitalized me every week, and I believe I wouldn't have sustained such high productivity for 18 months without it. I am grateful for my friendships with Tayler, Maria Paz, Elyssia, Eva, Alessandro, Ricco, Andrea, Houssam, José, Mammae, Hector, and Katrina.

Table of Contents

Dedication v

Acknowledgements vi

Table of Contents ix

Chapter 1. Introduction and Overview 1

Chapter 2. Background 6

2.1 Anastomosis 6

2.2 Polymer Hydrogels 8

2.3 Electroadhesion 10

2.4 Characterizing Gels and Tissues by Tensile Testing 11

2.5 Characterizing Gels and Tissue by Rheology 12

2.6 Characterizing Gel-Tissue Adhesion by Pull-Off Testing 13

2.7 Flow Test to Characterize Repaired Tissue 15

Chapter 3. Anastomosis Repair by Sleeve and Electroadhesion 17

3.1 Introduction 17

3.2 Results and Discussion 19

3.3 Conclusion 33

3.4 Experimental Methods 34

Chapter 4. Conclusions & Recommendations 38

4.1 Conclusions 38

4.2 Recommendations 39

References 41

Chapter 1: INTRODUCTION & OVERVIEW

Electroadhesion (EA) is a phenomenon that was discovered in 2010 by Asoh and Kikuchi.[1,2] The researchers experimented with cationic (G^+) and anionic (G^-) hydrogels. When the two gels are placed in contact, they do not adhere. However, when the gel pair is exposed to a DC electric field (10 V) for 10 to 20 s, the gels become strongly adhered, and we refer to this phenomenon as EA (Figure 1.1A). The adhesion persists even after the field is removed. Moreover, if the adhered gels are then placed in the same DC field with a reversed polarity, EA is reversed and the two gels can be detached (Figure 1.1B).

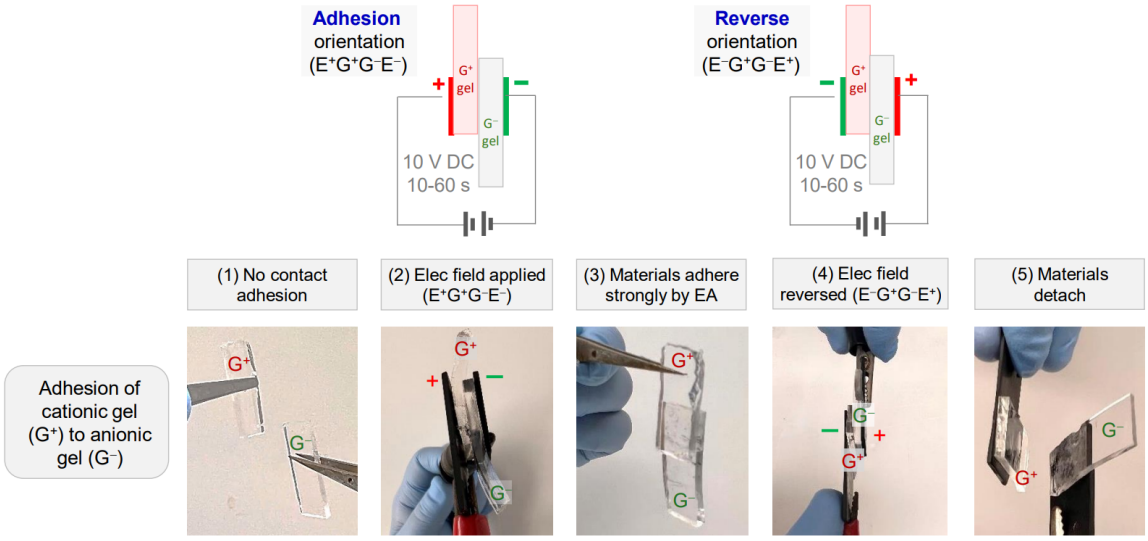


Figure 1.1. Electroadhesion (EA) of a cationic and an anionic hydrogel. A DC voltage of 10 V is applied for 10 s to the pair in the configuration shown. The gels get strongly adhered. When the polarity of the field is reversed, the gels can be detached.

Recently, our lab discovered that EA can also arise between a cationic gel and animal tissue.[3] Figure 1.2 shows EA of a cationic gel to a slice of salmon using the same

electrical configuration as in Figure 1.1 (10 V DC for 20 s). Note that only cationic gels (G^+) can be adhered by EA to tissues, which are known to have anionic character and are hence denoted as T^-. The mechanism for EA, both gel-gel (G^+/G^-) as well as gel-tissue (G^+/T^-), is expected to involve electrophoretic migration of cationic and anionic chain segments across the respective interfaces. These chain segments will then become bound and entangled by electrostatics, leading to adhesion.

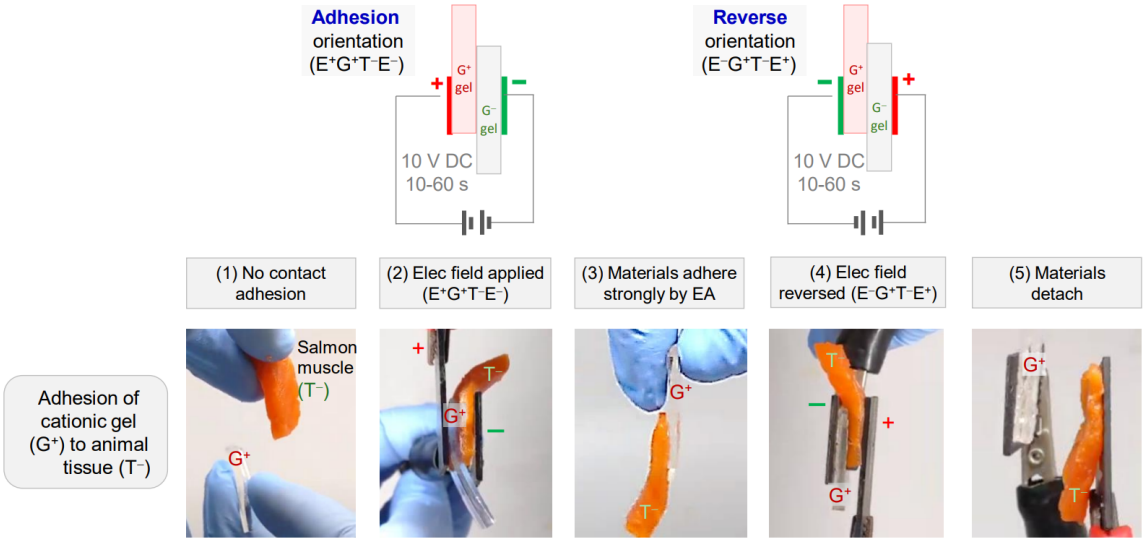


Figure 1.2. Electroadhesion of a cationic gel to animal tissue. (A) A cationic gel (G^+) is contacted with salmon (T^-) under a DC voltage of 10 V for 20 s. This results in strong adhesion. When the polarity of the field is reversed, the gel can be easily detached from the salmon.

An obvious application of gel-tissue EA is in surgery. That is, could we electroadhere a gel as a patch over cuts or tears in tissue? Currently, surgical repairs of torn tissue are done by suturing the torn edges together until the wound heals naturally. However, using sutures to close a wound can be cumbersome and requires considerable skill on the part of a surgeon. We therefore set out to explore the use of EA as an alternative

to suturing. In our previous work, we conducted in vitro experiments with animal (chicken) tissues and made *minor injuries* (2-4 mm cuts) in the tissue. Thereafter, we used EA to adhere gel patches over the cuts and showed that the tissues could indeed be repaired this way without sutures.

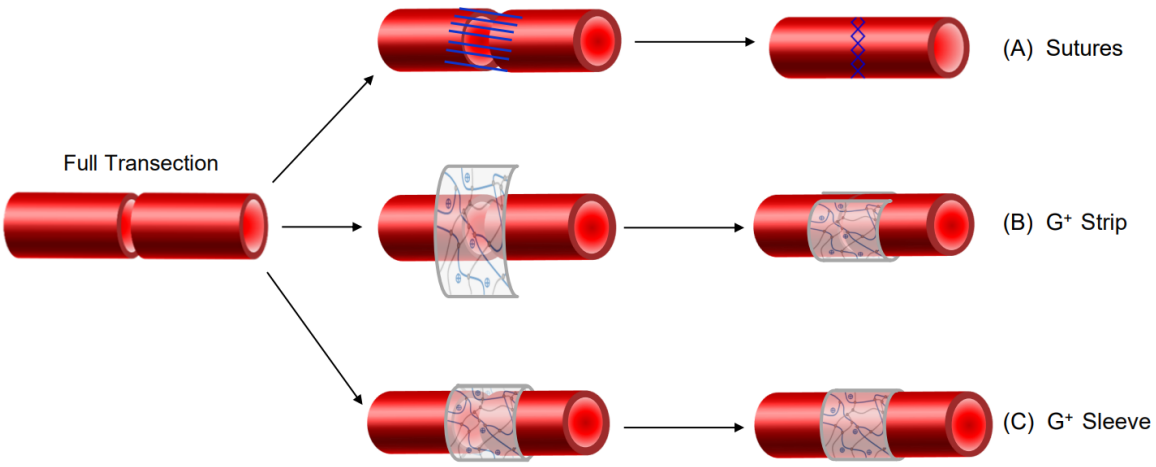


Figure 1.3. Anastomosis of a transected tube in the body (blood vessel or intestine). This is typically performed using sutures (A). In this study, we explore the use of electroadhesion (EA) of a cationic gel for anastomosis. Two modes are studied. (B) In one case, a long gel strip is wrapped around the cut pieces and attached by EA. (C) In a second case, a gel sleeve (hollow tube) is slid over the cut pieces and then attached by EA. The latter approach is shown to be better in this thesis.

In the present study, we are interested in using EA to repair *severe injuries*. One example of a severe injury is where a tubular tissue in the body (e.g., a blood vessel or an intestine) is cut into two segments. The surgical procedure of joining the segments is termed an *anastomosis*.[4] Thus far, surgical anastomosis in the clinic has only been done with surgical sutures or surgical staples.[5] While these techniques are generally regarded as standard practice, they carry inherent risks, including the potential for life-threatening postoperative complications, such as anastomotic leakage.[6-9] Anastomotic leakage occurs

when bodily contents escape out at the connection point, leading to subsequent infection.[8] Over one million anastomoses are performed annually in the United States, but anastomotic leakage is reported to occur in approximately 10% of patients.[9,10] This postoperative complication carries substantial consequences, including increased mortality and morbidity rates and prolonged hospitalization.[8,9] Such complications can increase healthcare costs for each patient by approximately $10,000. [11] In addition, the use of sutures or staples can prove to be difficult if the patient is either very young or very old. In both these cases, the tissue may be too soft or fragile, making it difficult to use these conventional procedures. For the above reasons, alternatives to sutures have been explored over the years in the form of surgical adhesives and sealants. However, no current adhesives are strong enough to perform a standalone anastomosis.

Here, we will examine the use of EA to perform anastomoses *in vitro* with animal tissues. We will discuss two ways to do this, as illustrated by Figures 1.3B and 1.3C. The first way is by using a long cationic gel *strip*, i.e., a rectangular segment with a length equal to the tube circumference and a width of about 5 – 10 mm. This strip is wrapped around the cut pieces for the repair (Figure 1.3B). A second approach is to use a cationic gel tube having a diameter close to that of the tubular tissue. We will refer to such a tube as a '*sleeve*' (Figure 1.3C). The sleeve is slipped over the two cut segments, as shown. In the cases shown in Figures 1.3B and 1.3C, after the strip or sleeve are in place, we apply 10 V DC for 20-60 s to induce EA between the gel and tissue.

To evaluate the effectiveness of these repairs, we conduct flow tests using a custom-built setup in the lab. Water (or another liquid) is flowed through the repaired tube at increasing pressures. The water pressure that induces the tube to burst (P_{burst}) is thereby recorded. We find systematic trends in P_{burst} as functions of gel strength, adhesion strength, etc. One key conclusion is that the gel-strips are not as effective as the gel-sleeves, i.e., P_{burst} is much higher with the latter. In experiments with sleeves and chicken intestines, we obtain P_{burst} values > 80 mm Hg, which is comparable to the fluid pressure *in vivo* in the intestines (whereas normal pressure in blood vessels ranges from 80-120 mm Hg).[12]

The findings reported in this thesis suggest that our newly designed sleeves, coupled with EA for adhering the sleeves to tissues, could be used to perform anastomoses effectively without the need for sutures. Thus, even the most severe tissue injuries could be repaired by EA without sutures or staples. In the future, we look forward to translating this technology for clinical use by surgeons.

Chapter 2: BACKGROUND

This Chapter will discuss anastomosis methods and how electroadhesion can be used in this regard. Then, we will discuss hydrogels and how they can be characterized. We will also discuss how gel-tissue adhesion can be quantified, both directly and indirectly, through burst-pressure measurements.

2.1. Anastomosis

Anastomosis refers to the rejoining of two disconnected pieces of tissue.[4] Anastomoses occur naturally in the body: for instance, arteries interconnect to facilitate circulation of blood and nutrients throughout the body.[7] A surgical anastomosis is an artificial connection made by a surgeon. These are frequently done with tubular tissues such as blood vessels (vascular anastomosis) or the intestines (gastrointestinal or GI anastomosis). An example of an anastomosis in the lab with a bovine aorta is shown in Figure 2.1. Ethicon Prolene 6-0 sutures are used to connect the segments together.

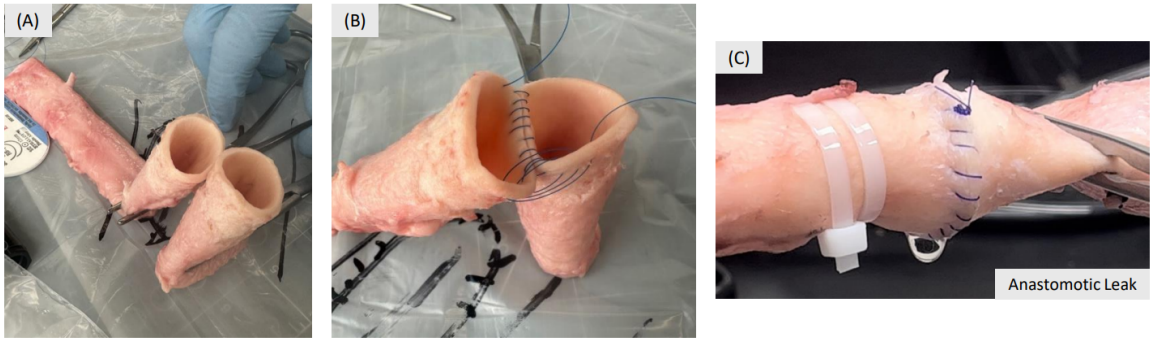


Figure 2.1. Anastomosis of transected bovine aorta using sutures. (A) Transected bovine aorta. (B) Connecting the two segments with Ethicon Prolene 6-0 sutures. (C) If the anastomotic joint is not perfectly sutured and sealed, fluid leaks out from it.

Anastomoses are commonly employed in bypass grafting, bowel resections, and organ transplantations. For example, in the case of an intestine, the surgeon may have to remove a segment that is injured, diseased, or occluded. The remaining parts are then connected together in an anastomosis using sutures or staples.[5] Sutures have long been the traditional choice for anastomosis. However, they carry the risk of several post-operative complications. One complication is anastomotic leakage, wherein the surgical connection (anastomotic joint) is imperfect. This failure is demonstrated in Figure 2.1C. We use our laboratory-scale flow setup to flow fluid through the sutured aorta, but fluid leaks out at the joint. In addition, there are several other disadvantages to sutures. Suturing is a time-intensive process that requires specialized training.[13] Moreover, sutures and staples often pose risks to those with delicate tissues, specifically in elderly and young patients.[14] For all these reasons, sutureless anastomosis repair is being explored using adhesives and sealants, but these are yet to reach the clinic.

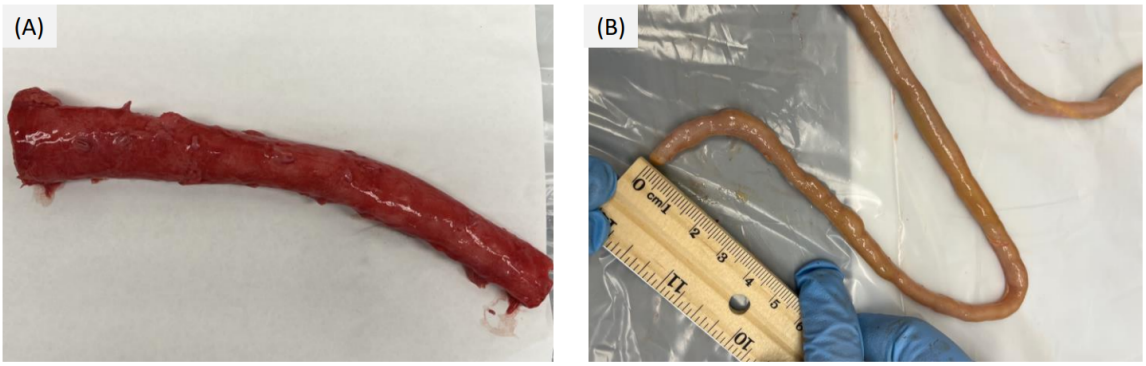


Figure 2.2 Tissues used in this study for *in vitro* anastomosis testing. (A) bovine aorta. (B) chicken small intestine.

The tissues we will aim to repair in the lab will be the aorta (from cows or pigs) and the small intestine (from chicken).[15] Figure 2.2 shows photos of these tissues. The aorta (Figure 2.2A) is a large artery with a diameter of 20 to 40 mm. It transports oxygen-rich blood from the heart to the rest of the body. The small intestine (Figure 2.2B) is the part of the digestive system where nutrients are absorbed from food.[16] It is a long tube with a contour length of 3 to 5 m and a diameter of 9 to10 mm. Note that these tissues are usually covered in fat when purchased from the butcher shop. This fat has to be removed before it can be used in our experiments.

2.2. Polymer Hydrogels

Hydrogels are three-dimensional networks of polymer chains swollen with water.[17,18] In these networks, the chains are crosslinked, either by covalent (chemical) bonds or non-covalent (physical) bonds.[17] A schematic of a gel is shown in Figure 2.3A. The average mesh size ξ of the gel ranges from 5 to 100 nm.

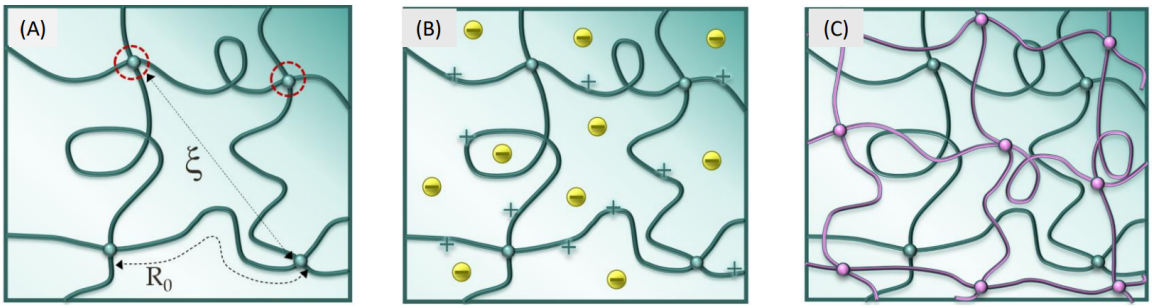


Figure 2.3. Schematics of hydrogels. (A) Schematic of a nonionic gel showing polymer chains crosslinked into a network. The network has a mesh size ξ and is swollen with water. (B) Schematic of a cationic gel with anionic counterions (shown in yellow). (C) Schematic of an interpenetrating network (IPN) where there are two distinct crosslinked polymer networks (shown in green and pink).

Chemically crosslinked gels are formed by free-radical polymerization of a monomer and a crosslinker. For example, a gel can be made by mixing the monomer acrylamide (AAm), the crosslinker N,N'-methylenebisacrylamide (Bis), the initiator ammonium persulfate (APS) and the accelerant tetramethylethylenediamine (TEMED) and allowing it to polymerize at room temperature. TEMED accelerates the decomposition of APS into free radicals.[19] These free radicals initiate the polymerization by binding to AAm monomers, allowing the monomers to link to each other and become polymer chains. Bis molecules then connect AAm chains resulting in crosslinking of the chains. The final result will be a crosslinked network, i.e., a gel of AAm.

To make the gel cationic, a cationic monomer such as quaternized dimethyl aminoethyl methacrylate (QDM) can be added to the recipe.[20] The QDM and AAm monomers will then copolymerize to form the chains in the network. The QDM/AAm molar ratio will dictate the charge density of the gel. A schematic of a cationic gel is shown in Figure 2.3B. Note that the cationic charge on the chains (e.g., due to amine groups) is balanced by anionic counterions (e.g., chloride, Cl^-).

Gels can be made stronger by incorporating a second network. [21-23] These gels are known as interpenetrating networks (IPNs) (see schematic in Figure 2.3C).[17] For example, in this study, we make an IPN of QDM (a chemical network) and gelatin (a physical network). Gelatin gels are formed by dissolving gelatin powder in water at approximately 40°C and cooling the hot solution. Upon cooling, strands of gelatin, which is a denatured protein, bind to each other and form triple-helical segments through non-covalent

interactions such as hydrogen bonding. [21,24,25] These segments act as crosslinks in the gelatin network.

2.3. Electroadhesion

Electroadhesion (EA) refers to adhesion that is induced by applying an electric field.[3] As discussed in Chapter 1, our lab discovered that EA can be achieved between cationic gels and biological tissues. Figure 2.4 lists all the tissues in mammals to which EA has been achieved; note that many different mammals have been tested in this regard. The list encompasses many of the important tissues in our body. These include arteries, intestines, trachea, and esophagus, all of which are tubular tissues that convey either blood, air, or digested food. Other adhering tissue types include muscle, tendon, cartilage, fascia, and cornea. Organs that show adhesion include the vital organs such as heart, stomach, liver, spleen, and bladder.

The mechanism for EA is yet to be entirely understood. It is believed to involve electrophoresis of oppositely charged chain segments across the interface.[26] Note that only cationic gels can be adhered to tissues. The anionic character of tissues is expected to arise either from polymers in the extracellular matrix (ECM), such as hyaluronic acid and mucin, or proteins attached to cell membranes.

Gel-tissue EA observed	
Artery	Cow, Pig, Mouse, Chicken, Human
Trachea	Chicken, Cow
Esophagus	Pig
Large Intestine	Mouse, Sheep
Small Intestine	Chicken, Pig
Skeletal muscle (T>L)	Cow, Pig, Mouse, Chicken
Tendon (T>L)	Cow
Cartilage (Hyaline)	Cow, Chicken, Pig
Fascia	Mouse, Pig
Cornea	Cow, Pig
Heart	Cow, Pig, Mouse, Chicken
Stomach	Mouse
Liver	Pig, Mouse, Chicken
Spleen	Pig, Mouse
Bladder	Pig

Figure 2.4. Biological tissues in mammals to which cationic gels can be adhered by EA. The tissue type is listed on the left, and the corresponding animals from which the tissues were tested are on the right. All EA experiments (10 V DC for 30 s) were done with the same cationic QDM gel.

2.4. Characterizing Gels and Tissues by Tensile Testing

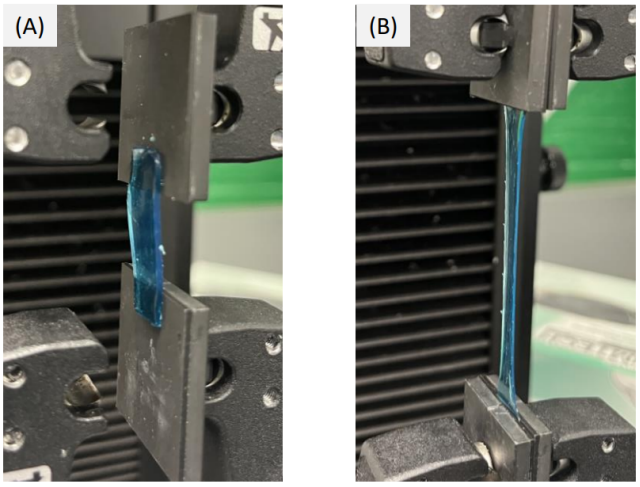


Figure 2.5. Photos of a tensile test on a gel. (A) The gel is placed between the clamps of an Instron. The bottom clamp is stationary, while the top clamp moves upward at a constant rate. (B) The stress needed to elongate the gel (to a certain strain) is measured. Thereby a stress-strain curve for the material can be obtained.

To assess the mechanical properties of gels and tissues, they are tested under tension using an Instron. In tensile testing, the material is clamped on both ends (Figure 2.5A). One end remains stationary, while the other is moved at a specified rate, thereby stretching the gel (Figure 2.5B). The force F the instrument has to apply to achieve this stretching is converted to a tensile stress $\sigma = F/A$, where A is the cross-sectional area of the sample. This stress can be plotted as a function of the tensile strain $\varepsilon = \Delta l/l$, where the original sample size is l and the change in size is Δl.

From a stress-strain plot, several parameters can be extracted. First is the Young's Modulus Y (or elastic modulus), which is the slope in the linear region of the plot at low strains.[27,28] Next is the tensile strength (TS), which is the highest stress that the material can withstand before it breaks. This quantity is also sometimes called the ultimate tensile strength (UTS). In cases where the stress increases monotonically with strain, TS is the same as the stress-at-break.[29] In other cases, the stress can reach a peak at the TS and then decrease before the material breaks. A third quantity is the strain-at-break ε (or elongation at break), which is the maximum extent to which the material can be deformed before it breaks.

2.5. Characterizing Gels and Tissues by Rheology

Rheology is another technique used to study gels and tissues. Rheological studies are usually conducted under dynamic oscillatory shear. Here the sample is deformed by a

sinusoidal strain $\gamma = \gamma_0 \sin(\omega t)$, where ω and γ_0 are the frequency and the strain amplitude. The stress response will also be sinusoidal and is written as follows:

$$\sigma = G'\gamma_0 \sin(\omega t) + G''\gamma_0 \cos(\omega t) \tag{2.1}$$

where G' is the *storage* or *elastic* modulus and G'' is the *loss* or *viscous* modulus. These measurements must be done in the *linear viscoelastic* (LVE) *regime* where the moduli are only functions of ω. The rheological signature of a gel is that its elastic modulus G' will be nearly independent of ω, and moreover, G' will be higher than G''. This indicates the elastic response of the gel. The value of G' quantifies the *stiffness* of the gel. The higher the density of crosslinks, the higher the G', i.e., the stiffer the gel.

2.6. Characterizing Gel-Tissue Adhesion by Pull-Off Testing

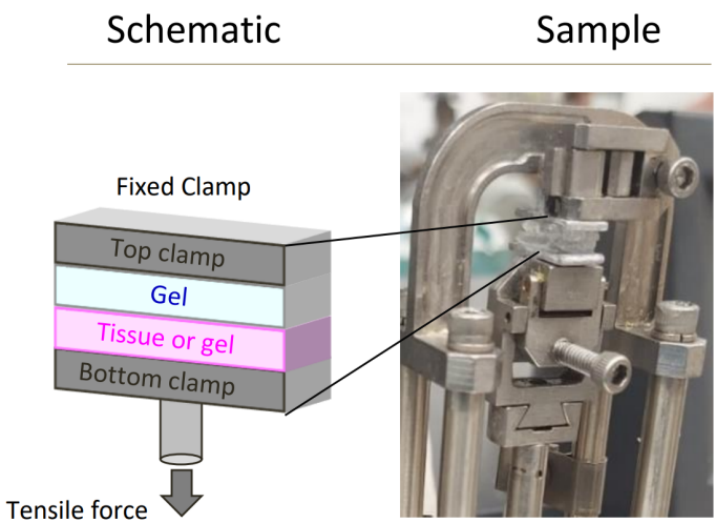


Figure 2.6 Pull-off testing to measure adhesion strength. Gel-tissue samples are superglued to the clamps. The bottom clamp is moved downward at a fixed rate. The stress required to detach the materials gives their adhesion strength.

Gel-tissue adhesion strength is measured by pull-off testing, which is conducted on a Dynamic Mechanical Analyzer (DMA).[30] The two materials are sandwiched between the clamps of the DMA, as shown in Figure 2.6. A cyanoacrylate glue (Super Glue) is used to secure the outward-facing side of the gel and tissue to the respective clamp. During the test, the top clamp remains stationary while the bottom clamp moves downward at a constant rate. The stress required to detach the adhered pair is a measure of the pull-off adhesive strength. A higher stress indicates stronger adhesion between the samples.

2.7. Flow Tests to Characterize Repaired Tissues

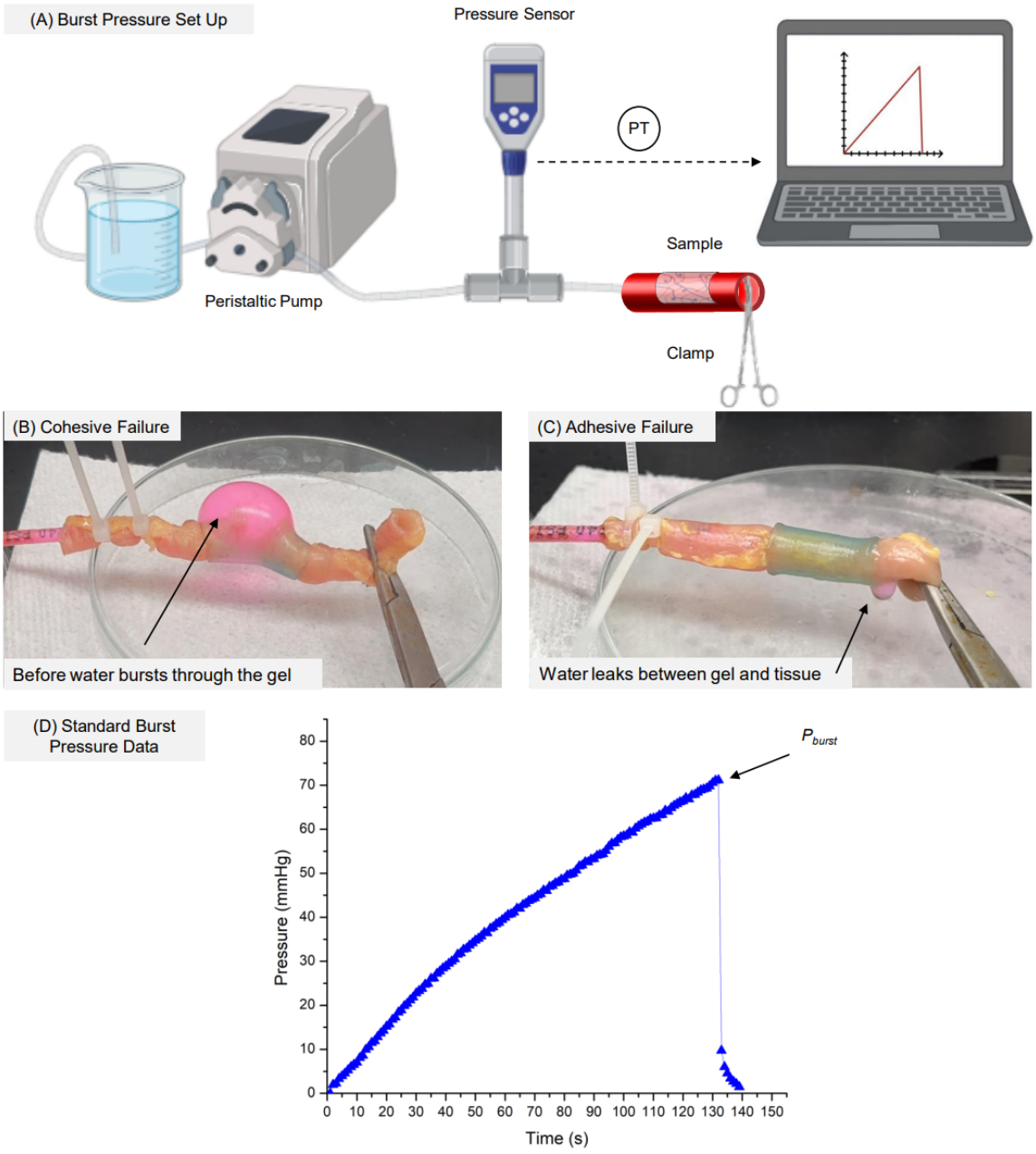


Figure 2.7. Burst pressure testing of repaired tubes. (A) Flow setup. (B) Cohesive (gel) failure: water bursts through gel. Gel is weaker than adhesion. (C) Adhesive failure: water seeps between tissue and gel. (D) Standard burst pressure graph. Pressure measured at failure equals burst pressure.

We have built a flow setup in the lab to test the success of an anastomotic repair.

In our tests, fluid is flowed through a repaired tube by a peristaltic pump, as shown in

Figure 2.7A. The pressure P of the fluid is measured by a pressure sensor. One end of the tube is clamped and thereby P in the tube keeps increasing. At some point, the fluid will break through the tube, and the P at this failure point is the burst pressure P_{burst}. Figure 2.7D shows a P vs time plot from the experiment. Beyond the failure point ($P = P_{burst}$), P drops to zero. Two modes of failure are observed in the testing: cohesive and adhesive. Cohesive failure (Figure 2.7B) arises when the adhesion strength surpasses the gel strength: if so, the fluid bursts through the gel. Conversely, adhesive failure occurs when the adhesion is weaker than the gel, leading to fluid seeping between the gel and tissue at their interface (Figure 2.7C).

Chapter 3: ANASTOMOSIS BY ELECTROADHESION OF GELS

3.1. Introduction

This study explores the use of electroadhesion (EA) to perform *in vitro* anastomoses with animal tissues. As models for tubular tissues, we will work with blood vessels, specifically the aorta from cows and pigs, as well as intestines from chickens. The tissues will be transected and we will attempt to rejoin the cut segments without using sutures. As discussed in Chapter 1, there are two ways of doing this with gels and EA. The first is using a cationic *gel strip* (Figure 1.3B) having a length equal to the tube circumference and a width of 5 – 10 mm. This strip will be wrapped around the cut pieces and we will apply the DC field to induce gel-tissue EA. A second approach is to use a cationic *gel sleeve* (Figure 1.3C). This will be slipped over the cut segments, after which we will again induce gel-tissue EA.

To increase the likelihood of success with our EA-based approach, we will first optimize the mechanical properties of the gel. That is, our gel must be (a) strong, i.e., it must have a high tensile strength *TS*; (b) elastic and stretchable, i.e., it must have a high elongation at break ε under tension; and (c) it must have a high adhesion strength σ_{adh} to the tissue under study. We will use a formulation for the gel that maximizes all three of these properties. The flexibility of the gel will be especially important for the repair of intestines. Note that intestines undergo peristalsis — an involuntary wave-like muscle movement that propels food and fluids through the gastrointestinal tract. The gel must hence flex together with the intestine (without losing adhesion) to allow for such peristalsis.

To evaluate the effectiveness of these repairs, we will conduct flow tests using a custom-built setup in the lab (as discussed in Section 2.8). Water will be flowed through the repaired tube and the burst pressure (P_{burst}) will be recorded. The mechanical properties of the gel (TS, ε) as well as the gel-tissue σ_{adh} will impact the value of P_{burst}. Our goal is to repair the tissue in a way that the tissue can resume normal functionality. In this context, for a repair to be regarded as successful, the repaired tissue must exhibit a P_{burst} that is comparable to those in the tissue *in vivo*. For the case of chicken intestines, when gel sleeves are used to perform an anastomosis, we find that $P_{burst} > 80$ mm Hg. This value is comparable to the fluid pressure *in vivo* in the intestines. Thus, our findings suggest that our newly designed sleeves, coupled with EA for adhering the sleeves to tissues, could be used to perform anastomoses effectively without the need for sutures.

3.2. Results and Discussion

3.2.1 Limitations of Gel Strips

Thus far, electroadhesion has successfully repaired minor tissue cuts with a gel patch. For severe injuries, the approach involves cutting a gel strip that matches the size of the cut. However, for tissue segments that are fully transected, simply electroadhering a gel strip around the circumference of the tissue presents immediate challenges. As depicted in Figure 3.1, the primary issue arises from the discontinuity of the gel strip, which leaves a section of the cut unsealed. Flow tests reveal that the repair fails at this juncture, where the gel proves ineffective in sealing the wound, leading to fluid leakage. This failure mode is attributed to the inherent geometry of the cationic gel strip, indicating its unsuitability for repairing this type of injury.

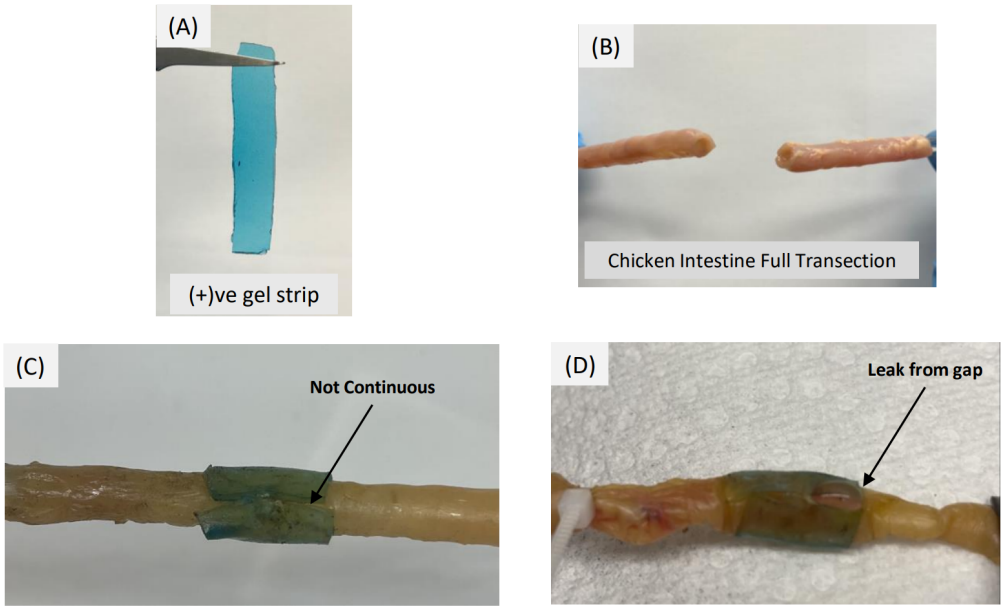


Figure 3.1. Anastomosis of chicken intestine by EA of a cationic gel strip. (A) Gel strip. (B) Transected chicken intestine. (C) Repair with gel strip results in a gap between the ends of the gel. (D) When fluid is flowed through the repaired tissue, water leaks from the gap.

Another issue with the gel strip is its inability to securely rejoin the two tissue segments. While the electric field induces strong adhesion between the gel and tissue, there is insufficient reinforcement from the gel to maintain the connection between the tissue segments. Proper healing requires the two halves of the tissue to remain in contact. Thus, a disadvantage of the gel strip is its failure to provide sufficient support to ensure a secure connection between the two tissue segments.

3.2.2 Sleeve Introduction

The sleeve is a hollow cylinder-shaped gel that connects two tubular tissues. It is made from the same standard tough cationic gel, which consists of two distinct polymer networks. The first is a chemical network made from copolymerizing quaternized dimethyl aminoethyl methacrylate (QDM) and Acrylamide (AAm) monomers with Bis(acrylamide) (Bis) crosslinker. The positive charge of the polymer network is due to the quaternary substituted nitrogen in QDM. The second network is a physical network made from the protein gelatin. This network is formed by heating gelatin to its melting temperature (37°C) and subsequently cooling it to room temperature.[24] The denatured proteins aggregate through hydrogen bonding upon cooling, forming triple-helical crosslinks.

The sleeve effectively addresses the two primary challenges encountered with the gel strip. First, the discontinuity of the gel strip leaves a section of the cut unsealed, a problem resolved by the sleeve's continuous structure. As a unified piece of gel, the sleeve can be slid over both tissue segments. Secondly, while the gel strip provides no additional force to secure the segments, the sleeve offers mechanical reinforcement. During the repair,

stretching the sleeve over the tissue imparts an elastic force, firmly securing the two segments together. This aspect will be further elaborated upon in Section 3.3.6.

3.2.3 Sleeve Synthesis

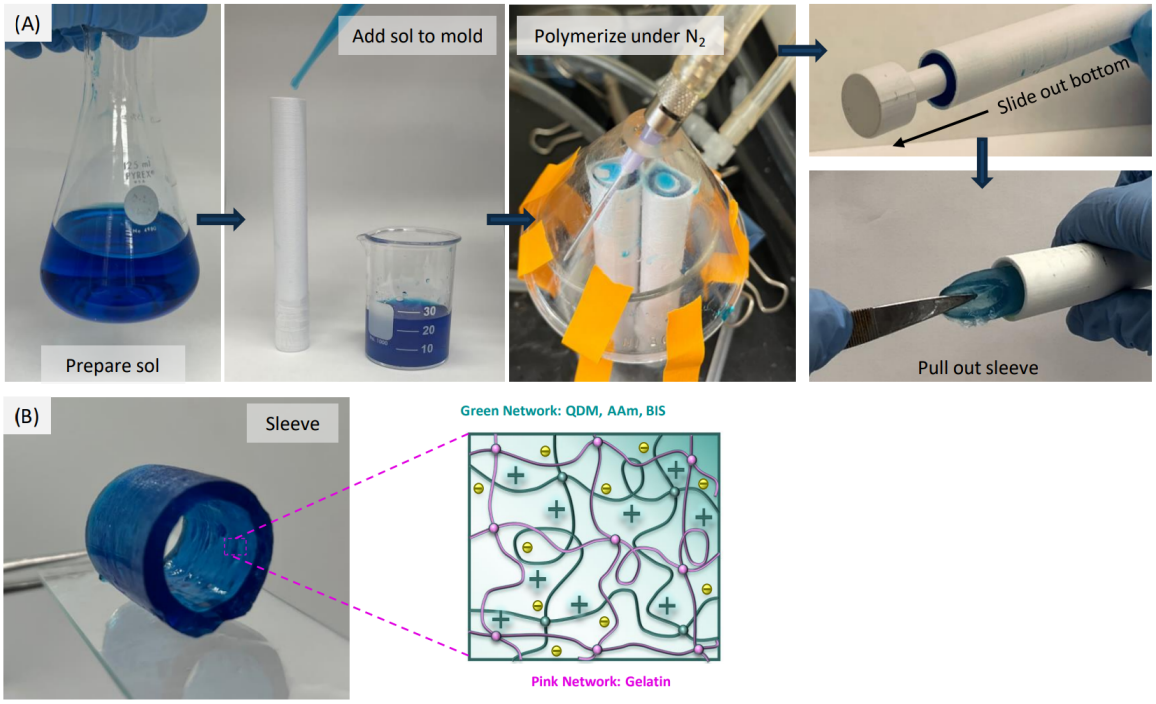


Figure 3.2. Synthesis of the cationic sleeve. (A) Prepare the sol by mixing Aam, QDM, and Bis in deionized water. After adding TEMED and APS, the solution is poured into the mold. Polymerize under Nitrogen for 2 hours. After polymerization is complete, the sleeve can be removed from the mold. (B) The gel has two polymer networks: a chemical crosslinked network of QDM, AAm, and Bis and a physical crosslinked gelatin network.

The molds are designed using Auto Fusion software, which enables the customization of dimensions. With control over mold dimensions, sleeves can be tailored to accommodate tissues of any size. Such versatility is advantageous as it expands the range of tissues that can be repaired. As illustrated in Figure 3.3, sleeves can be produced small enough to fit mouse intestines (4 mm) but can also be scaled up to accommodate larger blood vessels, such as bovine aorta (40 mm).

For the sleeve to serve as a successful suture-less anastomosis method, it must be (a) strong, i.e., it must have a high tensile strength *TS*; (b) elastic and stretchable, i.e., it must have a high elongation at break ε under tension; and (c) it must have a high adhesion strength σ_{adh} to the tissue being repaired.

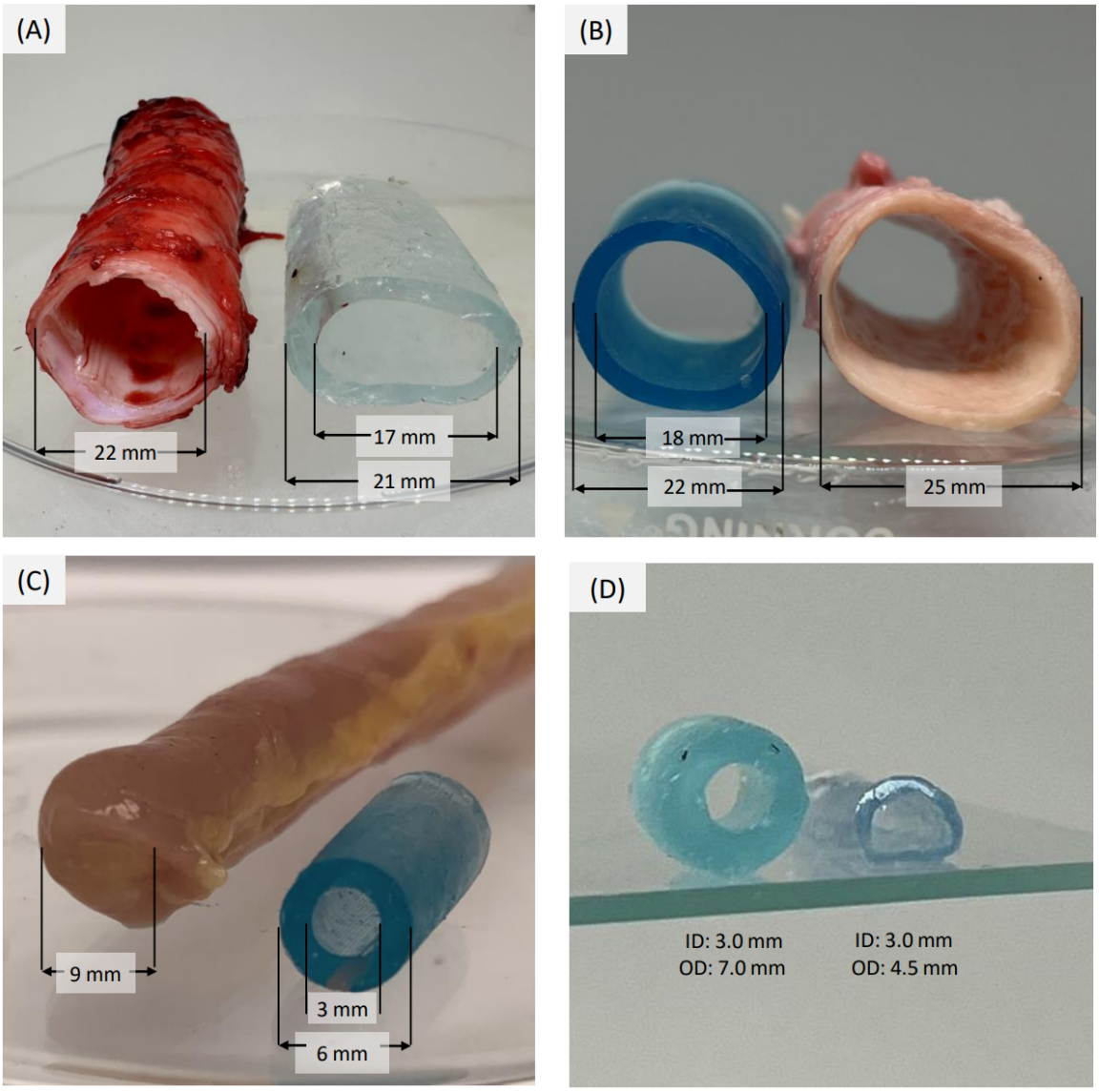


Figure 3.3. Dimensions of sleeve can be customized to fit various tissue types. (A) Sleeve for bovine aorta. (B) Sleeve for swine trachea. (C) Sleeve for chicken intestine. (D) Sleeves for small intestine in mouse

3.2.4 Sleeve Material Properties

The sleeve's elasticity is critical for its performance in surgical applications. The sleeve's stretchability is first demonstrated in Figure 3.4. Here, we reveal that the sleeve can be stretched approximately 3x its diameter in both the x and y-axes. This property is essential for repair, wherein the sleeve must be stretched over the tissue. Such stretchability demonstrates the sleeve's robustness and ability to withstand significant strain without failure.

In addition to its functionality in surgery, it is valuable to demonstrate the practicality of the sleeve from a clinical standpoint. As illustrated in Figure 3.4D, the size of the aorta decreases with increasing distance from the aortic valve. The aorta shown here reduces by approximately 20 mm in diameter from end to end. Despite these significant variations in aorta dimensions, we show that the sleeve can be stretched to accommodate any size segment of the aorta. This versatility is particularly advantageous in clinical settings, where a single-size sleeve can fit all patients, eliminating the need for patient-specific dimensions.

Furthermore, the sleeve's stretchability can be quantified using Instron. Figure 3.5 displays data from tensile tests, comparing the gel's and tissue's mechanical properties. Tissues are inherently robust materials, whereas hydrogels are characteristically soft materials. In terms of the sleeve's ability to achieve successful anastomosis, the gel must demonstrate a tensile strength adequate to withstand fluid pressure similar to *in vivo* conditions. We will confirm that the sleeve is sufficiently tough in Section 3.3.6.

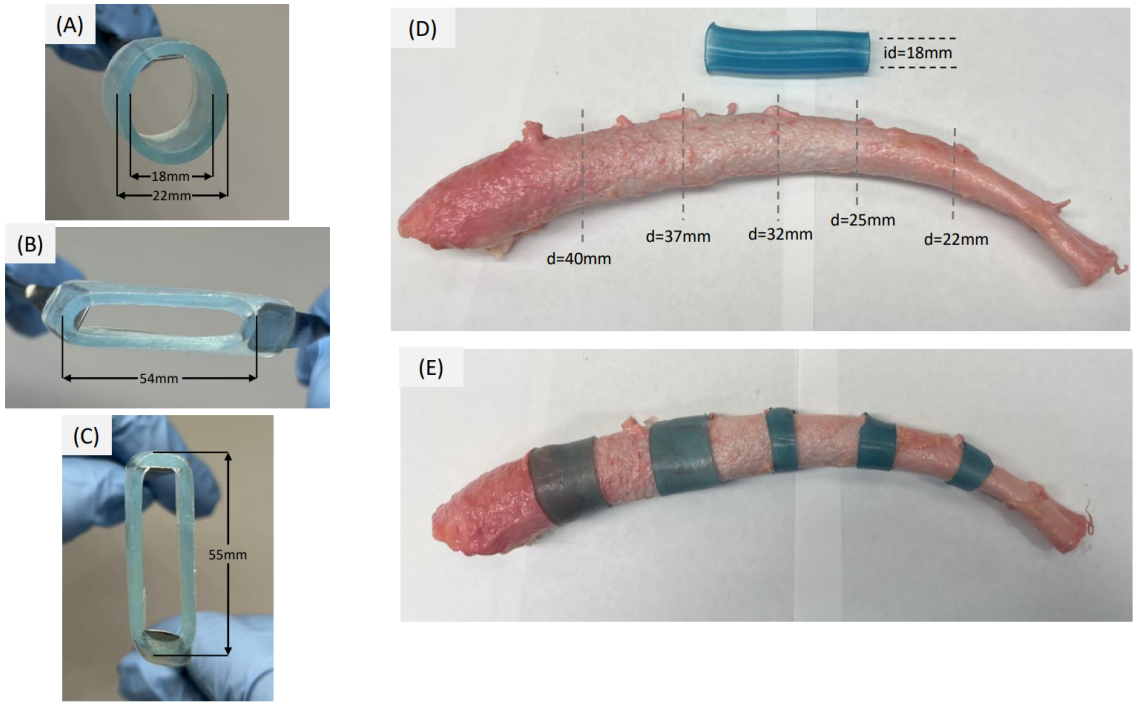


Figure 3.4. The sleeve can be stretched to fit a wide range of tissue diameters. (A) Unstretched QDM gel sleeve. (B) QDM gel sleeve stretched along the x-axis. (C) QDM gel sleeve stretched along the y-axis. (D) Aorta diameter is variable along its full length. (E) A gel sleeve, designed with a diameter of 18 mm, is capable of being stretched to fit a wide range of aortic diameters.

Furthermore, assessing the strain properties of the gel in comparison to those of the tissue holds significant importance. Strain is defined as a measure of the material's capacity to stretch. As illustrated in Figure 3.5B, the gel's strain-at-break is more than double than that of the tissues. Consequently, after the sleeve is employed to repair the tissue, peristalsis will not be hindered by the sleeve, i.e., the sleeve will have the ability to stretch and move with the surrounding tissue.

To ensure that the sleeve does not impede fluid flow, we characterize the elastic modulus of both gel and tissue. Elastic modulus is a measure of a material's stiffness. In Figure 3.5D, it is shown that the aorta is more than 2x stiffer than the gel, confirming the

sleeve's flexibility to move with the surrounding tissue. Consequently, the sleeve acts as a flexible structure, allowing tissue expansion and normal fluid flow without constriction.

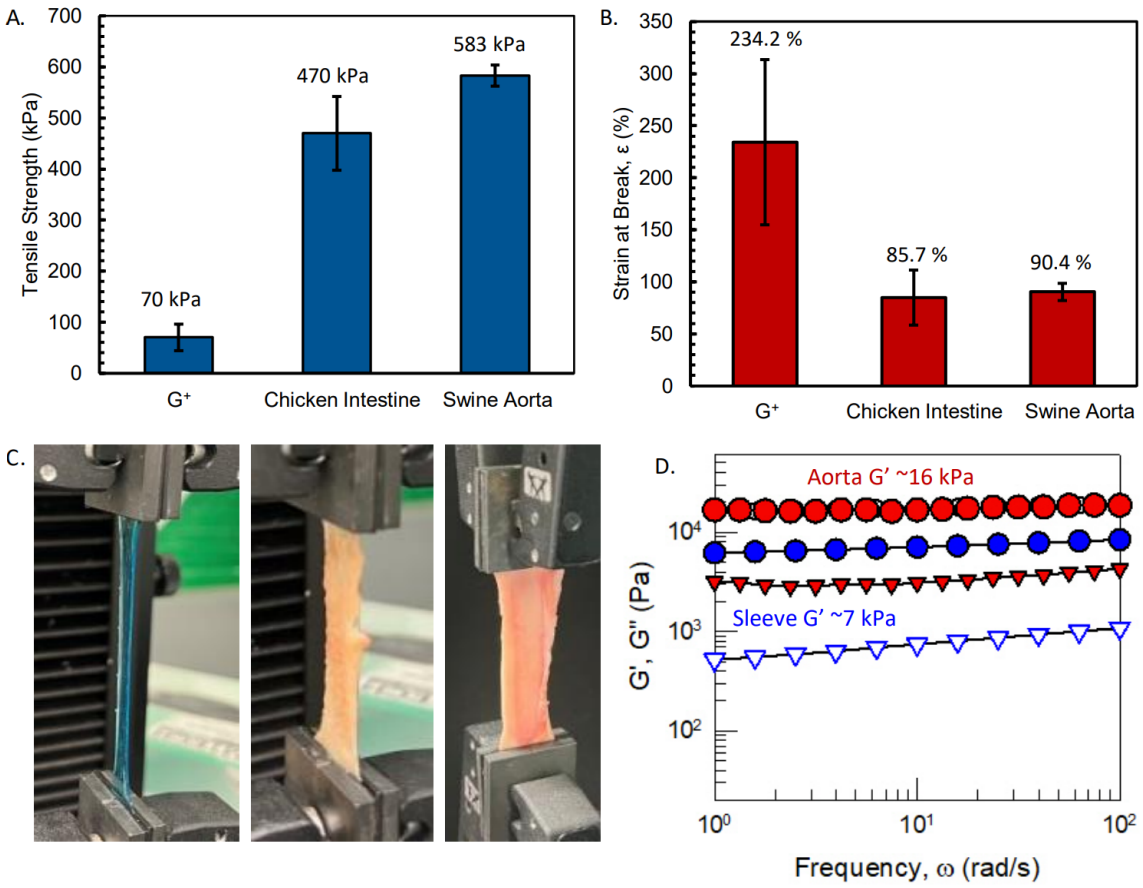


Figure 3.5. Mechanical properties of gel and tissues. (A) Tensile strength of gel, chicken intestine, and swine aorta. (B) Strain at break of gel, intestine, and aorta. (C) Gel and tissue samples during tensile testing. (D) Comparing rheological data for gel and aorta.

3.2.5 Anastomosis of Aorta by Electroadhesion of the Sleeve

Vascular anastomoses involve the repair of blood vessels, with the aorta serving as our model for testing anastomosis using sleeve and electroadhesion. Following the removal of fat from the aorta, the injury (full transection) is inflicted on the blood vessel, as depicted in Figure 3.6. Then, the repair is initialized by first slipping the two segments of the aorta into the sleeve and applying an electric field to induce adhesion between gel and tissue.

It's important to note that the "sandwich" electrical configuration is utilized, positioning the tissue and gel between the two electrodes. Achieving this setup requires the negative electrode to be endoscopically positioned inside the aorta while the positive electrode is placed externally on top of the sleeve.

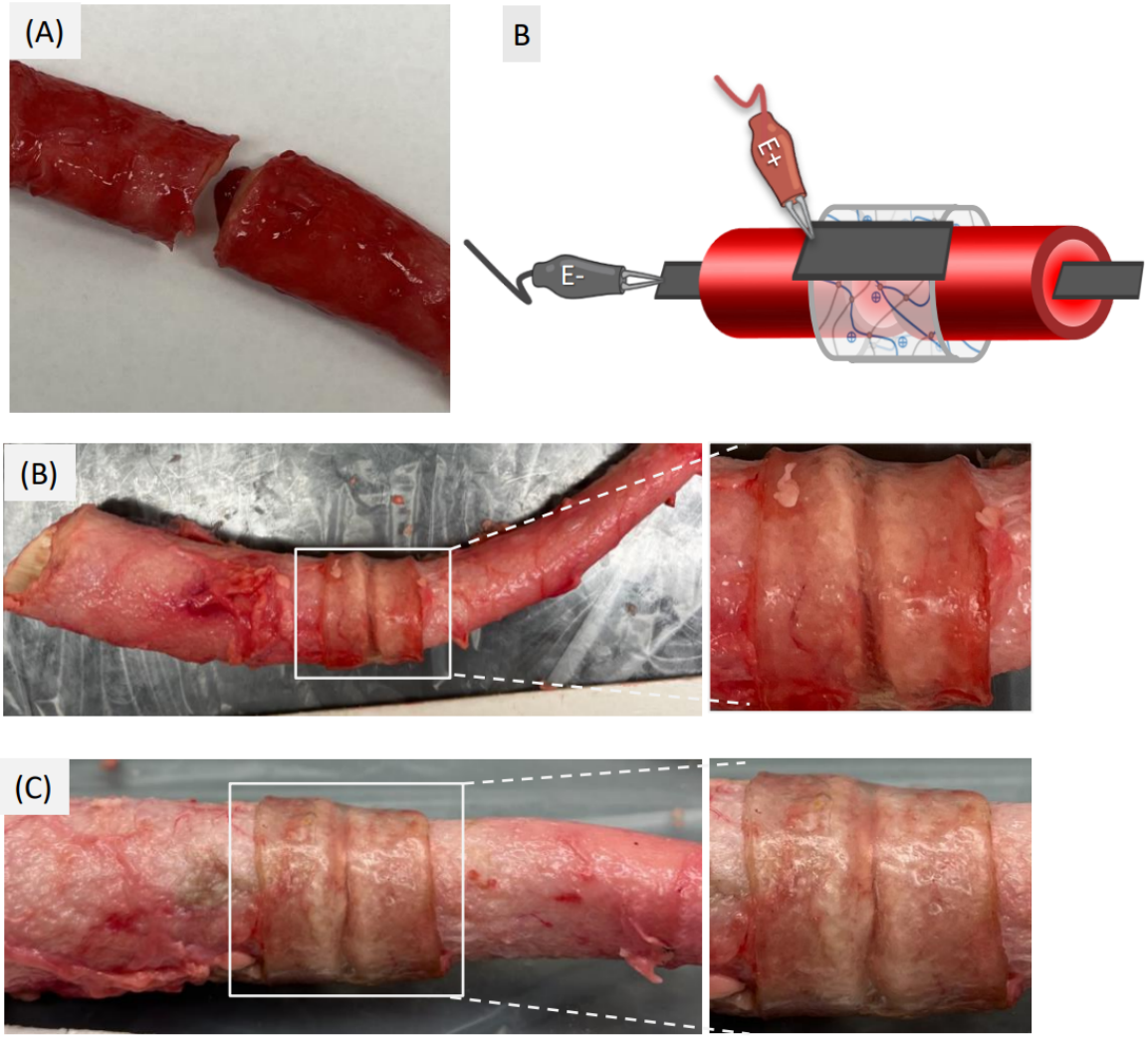


Figure 3.6. Anastomosis of transected bovine aorta by electroadhesion of the sleeve. (A) Fully transected aorta (B) Electrical configuration for anastomosis repair. The negative electrode is positioned endoscopically on the inside of the blood vessel and the positive electrode remains on the outside and is positioned atop of the sleeve. Electroadhesion was done using DC (20 V) for 30 seconds at each point along the circumference of the sleeve. (C) Repair before electric field. Note that though the aorta segments are inside the sleeve they are not in contact. (D) Repair after electric field. Aorta segments are now in contact and securely reconnected inside the sleeve.

Proper healing requires the two tissue segments to remain in contact. When the electric field is applied to the tissue, it secures the two segments together. In the absence of the electric field, adhesion between the tissue and gel is insufficient, allowing the tissue to move freely within the sleeve. This raises the risk of the tissue slipping out of the sleeve entirely. Figure 3.6 shows a gap between the two aorta ends before the electric field application. However, following the application of the field, the gap is closed as the segments are secured together, reinforced by the gel's strong adhesion to the tissue.

Pull-off tests are performed to characterize the adhesion strength of cationic gel to the aorta. Here, we measured the ultimate tensile strength— the stress required to separate the gel and tissue at the interface. To evaluate the adhesion attributable to the electric field, we compared electroadhesion samples to a negative control group labeled "Contact," consisting of gel-tissue pair samples not exposed to the electric field. As depicted in Figure 3.7A, all gel-tissue pairs subjected to the electric field exhibited higher tensile strength than those without exposure to the electric field. Therefore, we can conclude that the electric field is essential for inducing a strong adhesion between the sleeve and tissue segments. This is critical for effective repair, as fluid will be less likely to leak out of the connection point if adhesion is strong.

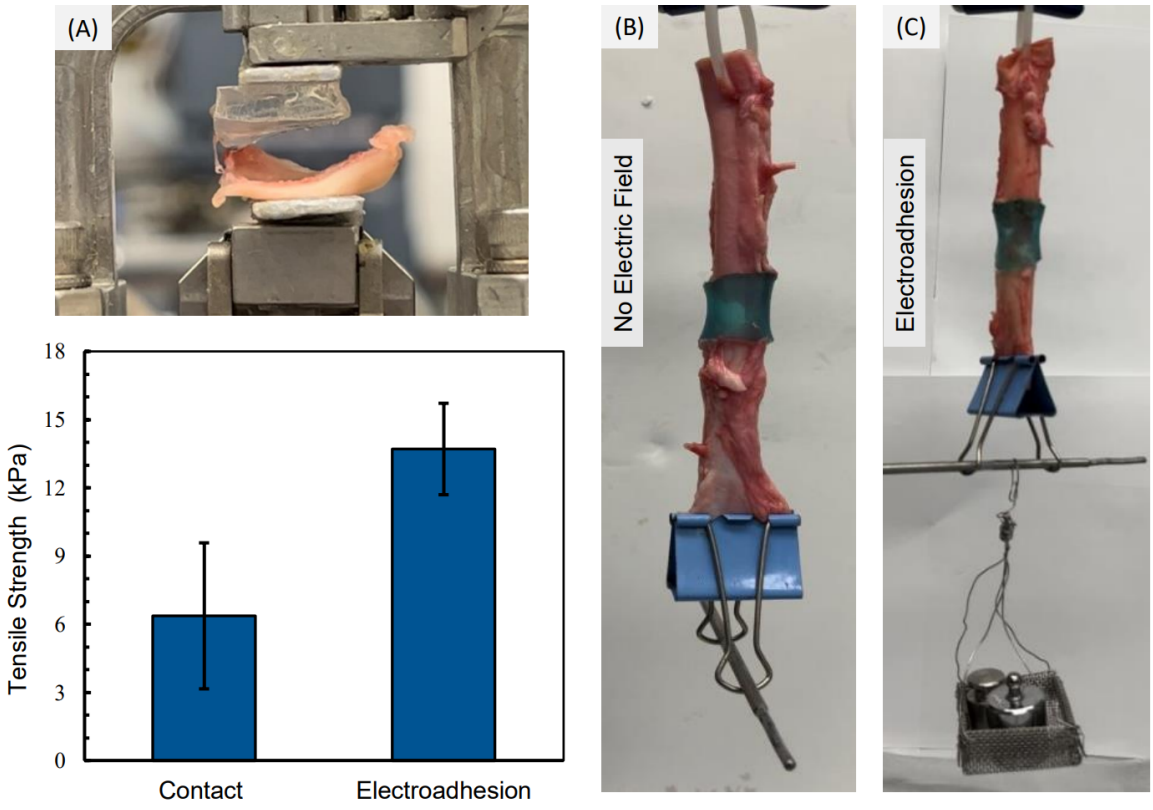


Figure 3.7. Characterizing gel-tissue adhesion strength by pull-off testing. (A) A pull-off adhesion test was conducted to compare gel-tissue samples adhered without and with the electric field. (B) Hanging weights from a fully transected aorta repaired by the sleeve without the electric field. The sample fails after being loaded with 28 g. (C) Hanging weights from a fully transected aorta repaired by the sleeve with the electric field. The sample fails after being loaded with 180 g.

The pull-off test is limited by its requirement for samples to be in a planar geometry. A distinguishing characteristic of the sleeve is its novel cylindrical geometry. In Figure 3.7, we devise an experiment to assess adhesion strength within this cylindrical context by suspending weights from the repaired tissue. Upon experimenting with tissues repaired by the sleeve without the electric field, we observe that the aorta segments are not securely held within the sleeve. The repair can only withstand the weight of the binder clip before the bottom half of the aorta slides out. In contrast, when the sleeve is used with the electric

field, it is capable of supporting a weight exceeding 100 g — significantly more than the aorta repaired without the electric field.

High adhesion strength is essential to prevent fluid leakage and to ensure a secure connection between the two aorta segments. Successful anastomosis entails rejoining the two tissue segments to restore fluid flow through the blood vessel and facilitate proper tissue healing. In this section, we have demonstrated the importance of the electric field in securely joining the two segments of the aorta.

3.2.6 Anastomosis of Intestine by Electroadhesion of the Sleeve

Gastrointestinal anastomosis pertains to the surgical reconnection of the small and large intestines. This investigation specifically targets small intestine repair. Following fat removal from the intestine, a full transection injury is induced, mirroring the procedure with the aorta. Prior to attaching the sleeve to the intestine, we ensure contact between the two intestinal segments. Figure 3.8 illustrates the electrical setup for executing electroadhesion. Plate electrodes are employed, with the negative electrode positioned endoscopically within the intestine, while the positive electrode remains externally positioned atop the cationic sleeve.

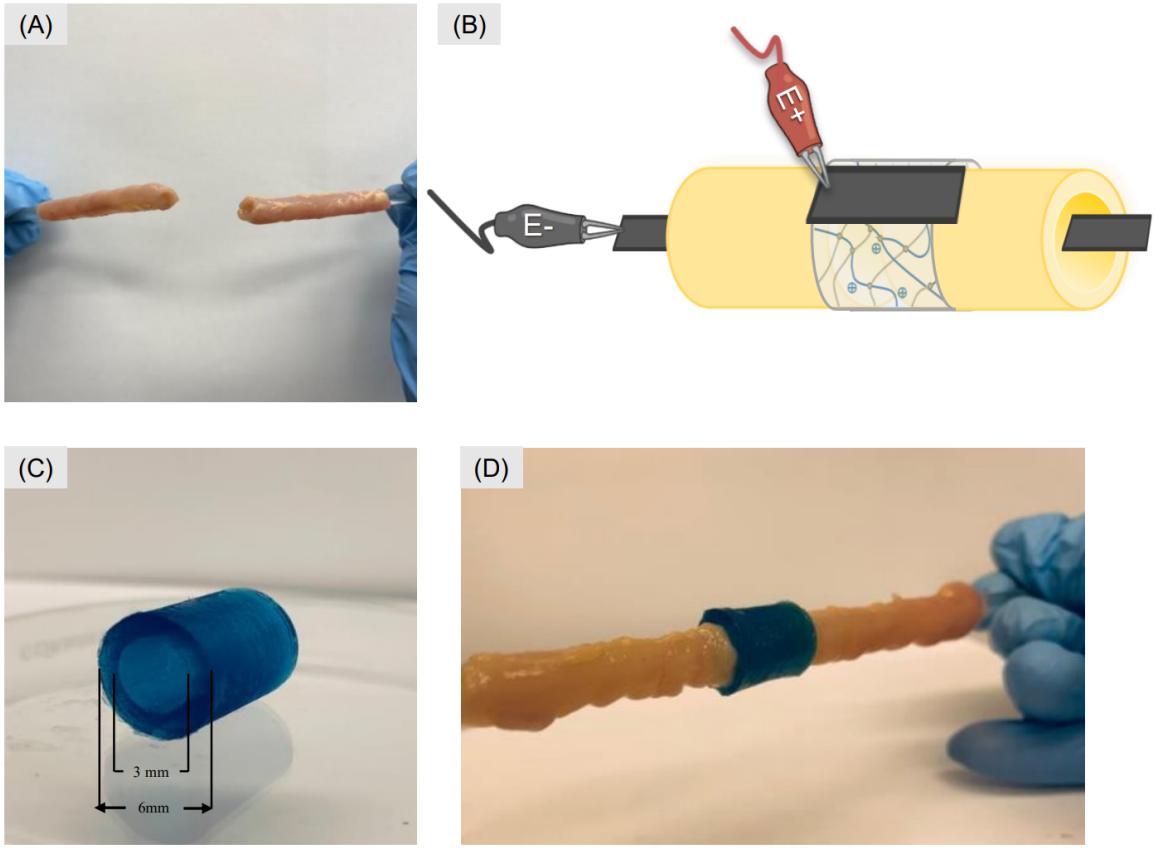


Figure 3.8. Anastomosis of transected chicken intestine by electroadhesion of the sleeve. (A) Fully transected chicken small intestine (B) Electrical configuration for anastomosis repair. The negative electrode is positioned endoscopically on the inside of the intestine and the positive electrode remains on the outside and is positioned atop of the sleeve. Electroadhesion was done using DC (20 V) for 30 seconds at each point along the circumference of the sleeve. (C) Sleeve used for the repair. (D) Repair after electric field. Intestine segments securely reconnected inside the sleeve.

As detailed in Section 3.3.2, one advantage of utilizing the sleeve over the gel strip lies in the sleeve's inherent geometry. To explore this, we prepared sleeves of varying diameters relative to the intestine to assess the impact of sleeve elasticity on repair. Given that the chicken intestine has a diameter of between 9 and 10 mm, we produced sleeves with diameters significantly smaller (4 mm), slightly smaller (7 mm), and equal (10 mm) to that of the intestine. To isolate the repair ability of the sleeve due to elasticity— no electroadhesion was done. Flow tests were conducted to determine the burst pressure

(P_{burst}) the repair could withstand before water leaked from the reconnection site. As shown in Figure 3.9A, the sleeve of the smallest diameter, or the sleeve that had to be stretched the most, could endure the highest P_{burst}. This confirms our earlier hypothesis that the sleeve's geometry alone contributes to reinforcing the two segments. Moreover, if the sleeve does not require stretching to fit over the intestine, the connection point between the two segments may remain unreinforced or even loose, leading to an increased risk of leakage.

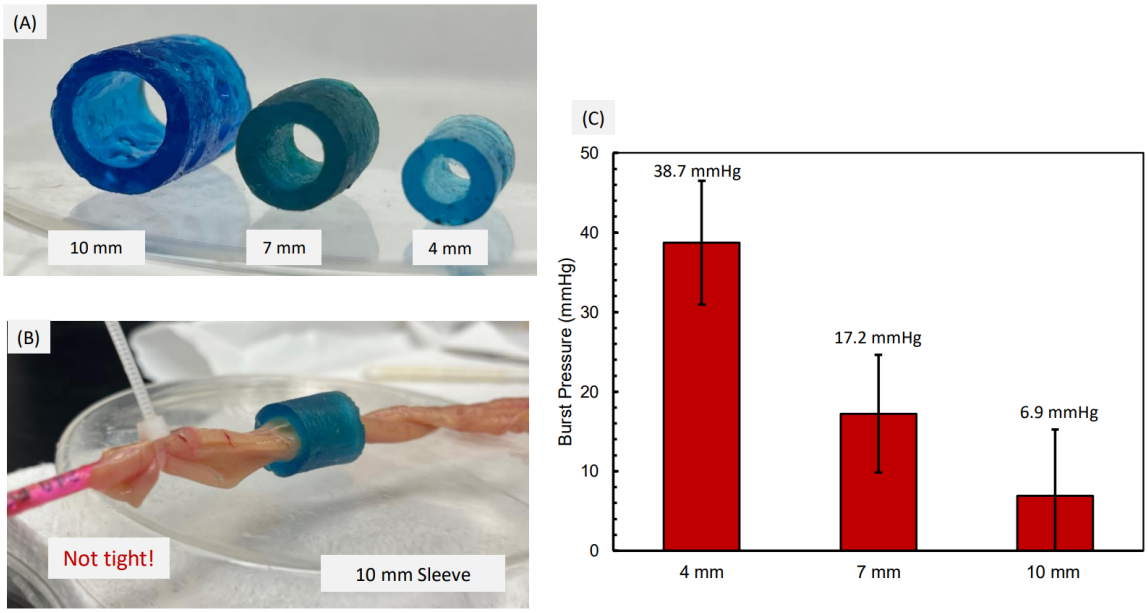


Figure 3.9. Evaluating the effect of sleeve size on burst pressure. (A) Sizes of sleeves used for full anastomosis repair of the small intestine. (B) Repair is conducted when the inner diameter of the sleeve matches that of the tissue being repaired. Note: The fit is not tight. (C) Pressures at which the sleeve failed—water leaked from the connection point.

Finally, we assess the efficacy of the initially proposed electroadhesion repair methods. These methods include electroadhering a long cationic gel strip and electroadhereing a cationic gel sleeve to two tissue segments. We conducted this variation of repairs on chicken intestines and evaluated their performance using our flow test setup.

Figure 3.10 presents a comparative analysis of each repair method's burst pressure. Our primary finding indicates that the sleeve alone (without the electric field) and the gel strip with electroadhesion produced comparable average P_{burst} values, falling within each other's standard deviation. Hence, we conclude that these two methods offer repairs of similar effectiveness. Additionally, our secondary finding illustrates that the sleeve with electroadhesion could withstand nearly twice the amount of fluid pressure compared to the other methods, establishing it as the most effective repair technique.

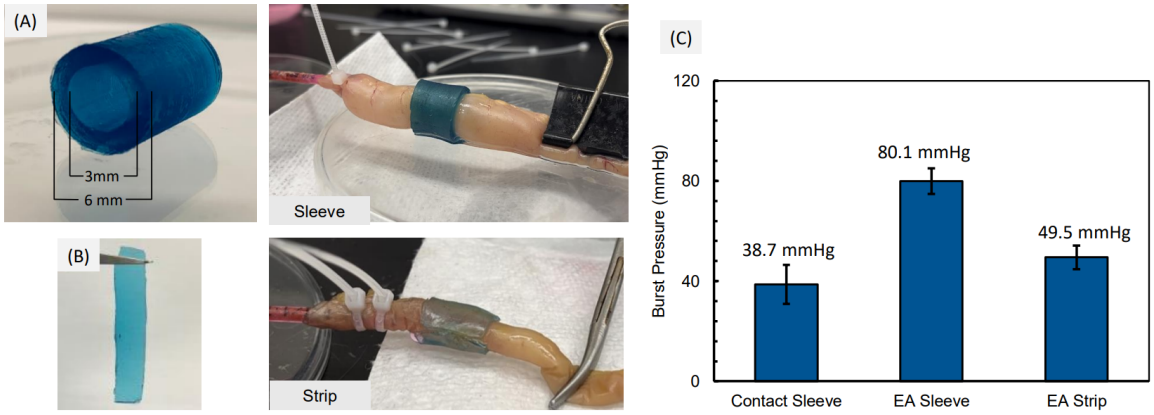


Figure 3.10. Burst pressure comparison of various electroadhesion repair methods. (A) Repair of the chicken intestine by sleeve without an electric field and picture of repair during flow test. (B) Repair of chicken intestine by strip with electric field and picture of repair during flow test. (C) Burst pressure data comparing sleeve without an electric field, sleeve with an electric field, and gel strip with the electric field.

In summary, our employment of flow tests enables us to model and evaluate the efficacy of each repair method in withstanding fluid flow through the intestine. We have demonstrated that the elasticity of the sleeve and the resultant force generated by its stretching play a substantial role in securing the connection between two disconnected tubular tissues. Furthermore, our findings reveal that electroadhering the sleeve to the

intestine results in the most successful repair, capable of withstanding fluid pressures comparable to those *in vivo*.

3.3 Conclusions

Previously, electroadhesion has demonstrated great success in repairing small cuts using a cationic gel patch. However, the limitations of a gel patch are revealed when attempting to repair more severe injuries, such as full transections. Simply electroadhering a gel strip around two tissue segments resulted in unsuccessful repairs, primarily due to challenges related to the geometry of the gel. These geometric issues prompted an exploration of alternative geometries better suited to this system. In particular, we investigated the efficacy of anastomosis repair using a gel with a hollow cylinder geometry, referred to as the sleeve.

The sleeve is a hollow cylinder-shaped gel designed for reconnecting two tissue structures. Utilizing the same tough cationic gel that has been effective in repairing small cuts in the chicken intestines, the sleeve's geometry is created by polymerizing the gel in custom PLA molds that were designed and 3D printed. The sleeve has been shown to possess superior stretchability, highlighting its adaptability to accommodate variations in tissue size among patients. Additionally, the sleeve exhibits greater flexibility, ensuring that tissues can resume normal functioning after repair and that the sleeve does not obstruct fluid flow.

Finally, we demonstrated the sleeve's capability to perform anastomoses on fully transected aorta and small intestine. The application of the electric field secures the connection following the stretching of the sleeve over the two tissue structures. Pull-off tests validate that the electric field substantially enhances the adhesion strength of the gel to tissue, a critical factor in preventing leaks and ensuring proper healing. This finding is further supported by the electroadhesion repair's ability to withstand a significant amount of weight. Additionally, anastomosis repair of the chicken intestine was evaluated using a flow test, yielding two primary conclusions: 1) the elastic force exerted by the sleeve reinforces the connection between the two tissue structures, highlighting the advantage of employing a sleeve that requires stretching over the tissue, and 2) anastomosis repair by sleeve and electroadhesion emerges as the most effective method compared to using a gel strip or sleeve contact alone.

3.4 Experimental Methods

Materials. The monomers Quaternized dimethyl aminoethyl methacrylate (QDM), Acrylamide (AAm), and the biopolymer Gelatin from swine skin were purchased from Sigma Aldrich. The crosslinker N, N'-methylene-bis(acrylamide) (BIS), accelerator N, N, N', N'-tetramethylethylenediamine (TEMED), initiator ammonium persulfate (APS), and Methylene Blue dye were purchased from Sigma Aldrich.

Sleeve Molds. Polylactic Acid (PLA) molds utilized for polymerization were 3D printed using AutoFusion software. This software offers full customization of all dimensions. Each sleeve mold consists of two printed prints. The first print resembles a piston, designed to

fit into a second print— a hollow cylinder. Once the polymerization process is complete, the piston print is gently removed, leaving behind a sleeve with a hollow core. Then, using forceps, the sleeve is separated from the second print.

Gel Sleeve Synthesis. Deionized water was bubble with Nitrogen for 30 minutes. To prepare cationic QDM gel, mix 20 wt% AAm, 4 wt% of QDM, and 0.018 wt% BIS into the deionized water. Next, add 2% of Gelatin to the solution and heat to 40°C for 10 minutes. Allow the solution to cool to room temperature and add 0.10 wt% TEMED and 0.18 wt% APS. Pour the solution into the molds and place them under Nitrogen gas to polymerize for 2 hours.

Tissue Preparation. The tissue used for testing was removed from all fat, and its internal contents were thoroughly washed out. Subsequently, full transection injuries were inflicted on the tissue.

Electroadhesion. For aorta anastomosis using the sleeve, the voltage was fixed at 20 V. Similarly, for small intestine anastomosis repair, the voltage was fixed at 20 V. Electroadhesion was performed using an Agilent DC power source (model E3612A), with graphite electrodes connected to the power source via alligator clips. The positive electrode was approximately 3 x 4 cm, while the negative electrode was approximately 2.5 cm x 7 cm. The negative electrode was positioned endoscopically within the small intestine, while the positive electrode remained external and was placed atop the sleeve. A schematic

illustrating the electrical configuration is provided in Figure 3.6. At each contact point, the electric field was applied for 30 seconds.

Tensile Testing. The Instron 6800 series was utilized to perform tensile testing. Tissue and gel samples were cut into 3 x 1 cm size strips. The samples were positioned in the center of both the top and bottom grips. The fixture separation distance was standardized to 15 mm, and the elongation rate used for all samples was 10 mm/min.

Rheological Testing. Rheological experiments were conducted on an AR2000 stress-controlled rheometer (TA Instruments) at 25°C using a parallel plate geometry (20 mm diameter). For the oscillatory shear (dynamic rheology) experiments, gel samples and tissues were cut into discs of 20 mm diameter and 3–4 mm thickness. Through stress-sweep experiments, the linear viscoelastic region of the samples was obtained, and a strain (1%) within this region was used to run the frequency-sweep experiments.

Pull Off Adhesive Testing. Pull-off adhesive strength was performed using a TA Instrument Q800 Dynamic Mechanical Analysis (DMA). Gel-tissue samples measured approximately 1 x 1 x 0.5 cm (length, width, thickness) in size. Gel-aorta samples underwent either electroadhesion using DC 20 V for 30 seconds or were placed in contact without exposure to the electric field (control group). Super glue was utilized to affix the outer-facing sides of the gel-aorta sample to the clamps. The cationic gel was secured to the top clamp, while the tissue was attached to the bottom clamp. Testing was performed with a pull-apart force of 0.5 N/min.

Flow Test Testing. Flow tests were conducted utilizing a Pharmacia-LKB peristaltic pump and a MadgeTech PRTemp pressure sensor. Water dyed with Rhodamine-6 served as the fluid for all experiments. Fluid flowrate was set to 100 mL/hour, and sample lengths were standardized to 6 cm. The flow test setup followed a linear configuration: the pump was positioned first, followed by the pressure sensor, with the sample located at the end and sealed with surgical clamps. Only pressure vs. time was recorded. For our purposes, temperature readings were disabled.

4: CONCLUSIONS & RECOMMENDATIONS

4.1. Conclusions

Anastomosis is a surgical technique used to reconnect transected blood vessels and intestines. Conventional anastomosis methods involve sutures and staples, but they carry inherent risks such as anastomotic leakage, bleeding, and infection that affects approximately 10% of patients. These challenges serve to drive the exploration of alternative anastomosis techniques.

In this thesis, we introduce an innovative approach: sleeve by electroadhesion. Prior work in our lab has shown that electroadhesion can be achieved between a cationic gel and tissue and has the capability to repair cuts in tissue. Here, we demonstrate that electroadhesion can repair fully transected tissue, the most severe injury, by redesigning the geometry of the cationic gel. Chapter III outlines the criteria for the sleeve to perform anastomosis: elasticity, flexibility successfully, and strongly adhere to the tissue.

Our study highlights the surgical and clinical applicability of sleeve elasticity. We demonstrated that the sleeve could accommodate significant variations in bovine aorta diameter, indicating that sleeve dimensions do not need to be tailored to individual patients. Tensile tests revealed that the sleeve has greater strain than the intestine and aorta. Flexibility characterization, using rheology, shows a lower elastic modulus than the aorta, ensuring the sleeve moves with tissue, not obstructing fluid flow post-repair. Pull-off tests

confirm strong adhesion to the tissue when the gel and tissue are exposed to an electric field.

However, satisfying these criteria alone does not guarantee successful anastomosis repair via electroadhesion by sleeve. Flow tests simulate *in vivo* conditions crucial for body channel tissue repair assessment. By performing flow tests, we found that the elastic force generated when stretching the sleeve over tissue aids in securing tissue segments together. Furthermore, we compared the burst pressures of the three sutureless methods introduced in Chapter I: electroadhesion by gel strip, sleeve with electroadhesion, and sleeve without electroadhesion. Our findings indicate that applying the sleeve with the electric field results in higher burst pressure, rendering it the most effective repair method.

4.2. Recommendations

In this study, we demonstrated the potential of the sleeve as a surgical technique for performing sutureless anastomoses. However, several aspects of the method require optimization before clinical adoption. Firstly, the electric configuration is crucial. Our results indicate that the electric field is pivotal in enhancing the adhesion strength between the sleeve and tissue. Therefore, refining the electrical aspects is essential to maximize the success of this tissue repair. Efforts should focus on finding an electrical configuration where both electrodes remain external or are positioned endoscopically.

Secondly, our research has shown that electroadhesion can be achieved within the interior of the aorta using the cationic gel. While we have demonstrated the sleeve's excellent stretchability, its compressibility remains a question. Can the sleeve be

compressed into a small unit and delivered endoscopically through the blood vessel to the injury site, enabling non-invasive repair from within the blood vessel?

Lastly, we have observed electroadhesion to the trachea, a structure similar in composition and architecture to the aorta but serving as an air passageway. While we have established the sleeve's efficacy in repairing blood vessels and intestines with liquid passage, exploring its application in repairing airways presents an intriguing direction for further research. Given the sleeve's potential as a sutureless alternative, these directions are vital to explore.

REFERENCES

[1] Asoh, T.-A.; Kawamura, E.; Kikuchi, A. "Stabilization of electrophoretically adhered gel-interfaces to construct multi-layered hydrogels." *RSC Advances* **2013**, *3*, 7947-7952.

[2] Asoh, T. A.; Kawai, W.; Kikuchi, A. "Alternating-current electrophoretic adhesion of biodegradable hydrogel utilizing intermediate polymers." *Colloids Surf B Biointerfaces* **2014**, *123*, 742-6.

[3] Borden, L. K.; Gargava, A.; Raghavan, S. R. "Reversible electroadhesion of hydrogels to animal tissues for suture-less repair of cuts or tears." *Nat Commun* **2021**, *12*, 4419.

[4] Thomas, M. S.; Margolin, D. A. "Management of Colorectal Anastomotic Leak." *Clin Colon Rectal Surg* **2016**, *29*, 138-44.

[5] Hintz, G. C.; Alshehri, A.; Bell, C. M.; Butterworth, S. A. "Stapled versus hand-sewn pediatric intestinal anastomoses: A retrospective cohort study." *J Pediatr Surg* **2018**, *53*, 959-963.

[6] Fabbi, M.; Hagens, E. R. C.; van Berge Henegouwen, M. I.; Gisbertz, S. S. "Anastomotic leakage after esophagectomy for esophageal cancer: definitions, diagnostics, and treatment." *Dis Esophagus* **2021**, *34*.

[7] Hyman, N.; Manchester, T. L.; Osler, T.; Burns, B.; Cataldo, P. A. "Anastomotic leaks after intestinal anastomosis: it's later than you think." *Ann Surg* **2007**, *245*, 254-8.

[8] Chiarello, M. M.; Fransvea, P.; Cariati, M.; Adams, N. J.; Bianchi, V.; Brisinda, G. "Anastomotic leakage in colorectal cancer surgery." *Surg Oncol* **2022**, *40*, 101708.

[9] Gessler, B.; Eriksson, O.; Angenete, E. "Diagnosis, treatment, and consequences of anastomotic leakage in colorectal surgery." *Int J Colorectal Dis* **2017**, *32*, 549-556.

[10] Saeidi, H.; Opfermann, J. D.; Kam, M.; Wei, S.; Leonard, S.; Hsieh, M. H.; Kang, J. U.; Krieger, A. "Autonomous robotic laparoscopic surgery for intestinal anastomosis." *Sci Robot* **2022**, *7*, eabj2908.

[11] Pollack, E.; Johnston, S.; Petraiuolo, W. J.; Roy, S.; Galvain, T. "Economic Analysis of Leak Complications in Anastomoses Performed with Powered versus Manual Circular Staplers in Left-Sided Colorectal Resections: A US-Based Cost Analysis." *Clinicoecon Outcomes Res* **2021**, *13*, 531-540.

[12] Mena, L. J.; Felix, V. G.; Melgarejo, J. D.; Maestre, G. E. "24-Hour Blood Pressure Variability Assessed by Average Real Variability: A Systematic Review and Meta-Analysis." *J Am Heart Assoc* **2017**, *6*.

[13] Olson, J. L.; Shandas, R.; Erlanger, M. "Development of a minimally invasive, injectable, shape memory suture and delivery system." *Ann Biomed Eng* **2012**, *40*, 1520-9.

[14] Horeman, T.; Meijer, E. J.; Harlaar, J. J.; Lange, J. F.; van den Dobbelsteen, J. J.; Dankelman, J. "Force sensing in surgical sutures." *PLoS One* **2013**, *8*, e84466.

[15] Li, H.; Gale, B.; Shea, J.; Sant, H.; Terry, C. M.; Agarwal, J. "Vascular Coupling System for End-to-End Anastomosis: An In Vivo Pilot Case Report." *Cardiovasc Eng Technol* **2017**, *8*, 91-95.

[16] Volk, N.; Lacy, B. "Anatomy and Physiology of the Small Bowel." *Gastrointest Endosc Clin N Am* **2017**, *27*, 1-13.

[17] Ahmed, E. M. "Hydrogel: Preparation, characterization, and applications: A review." *Journal of Advanced Research* **2015**, *6*, 105-121.

[18] Karoyo, A. H.; Wilson, L. D. "A Review on the Design and Hydration Properties of Natural Polymer-Based Hydrogels." *Materials (Basel)* **2021**, *14*.

[19] Giz, A.; Çatalgil-Giz, H.; Alb, A.; Brousseau, J.-L.; Reed, W. F. "Kinetics and Mechanisms of Acrylamide Polymerization from Absolute, Online Monitoring of Polymerization Reaction." *Macromolecules* **2001**, *34*, 1180-1191.

[20] Dragan, E. S.; Dinu, M. V.; Ghiorghita, C. A.; Lazar, M. M.; Doroftei, F. "Preparation and Characterization of Semi-IPN Cryogels Based on Polyacrylamide and Poly(N,N-dimethylaminoethyl methacrylate); Functionalization of Carrier with Monochlorotriazinyl-β-cyclodextrin and Release Kinetics of Curcumin." *Molecules* **2021**, *26*.

[21] Xing, Q.; Yates, K.; Vogt, C.; Qian, Z.; Frost, M. C.; Zhao, F. "Increasing mechanical strength of gelatin hydrogels by divalent metal ion removal." *Sci Rep* **2014**, *4*, 4706.

[22] Yasuda, K.; Ping Gong, J.; Katsuyama, Y.; Nakayama, A.; Tanabe, Y.; Kondo, E.; Ueno, M.; Osada, Y. "Biomechanical properties of high-toughness double network hydrogels." *Biomaterials* **2005**, *26*, 4468-75.

[23] Sun, X.; Liang, Y.; Ye, L.; Liang, H. "An extremely tough and ionic conductive natural-polymer-based double network hydrogel." *J Mater Chem B* **2021**, *9*, 7751-7759.

[24] Jaipan, P.; Nguyen, A.; Narayan, R. J. "Gelatin-based hydrogels for biomedical applications." *MRS Communications* **2017**, *7*, 416-426.

[25] Eysturskarð, J. "Mechanical Properties of Gelatin Gels; Effect of Molecular Weight and Molecular Weight Distribution." 2010.

[26] Asoh, T. A.; Kikuchi, A. "Electrophoretic adhesion of stimuli-responsive hydrogels." *Chem Commun (Camb)* **2010**, *46*, 7793-5.

[27] Nicholas, T. "Tensile testing of materials at high rates of strain." *Experimental Mechanics* **1981**, *21*, 177-185.

[28] Johnson, B. D.; Beebe, D. J.; Crone, W. C. "Effects of swelling on the mechanical properties of a pH-sensitive hydrogel for use in microfluidic devices." *Materials Science and Engineering: C* **2004**, *24*, 575-581.

[29] Drury, J. L.; Dennis, R. G.; Mooney, D. J. "The tensile properties of alginate hydrogels." *Biomaterials* **2004**, *25*, 3187-3199.

[30] Storage, T. M.; Brockman, R. A.; Tienda, K. M. "Analysis of Data Reduction Strategy used in TA Instruments Q800 DMA Test System," AIR FORCE RESEARCH LAB WRIGHT-PATTERSON AFB OH MATERIALS AND MANUFACTURING …, 2013.